Temperature Gradients in HPLC Columns Due to Viscous Heat Dissipation

H. Poppe/J. C. Kraak/J. F. K. Huber*

Laboratory for Analytical Chemistry, University of Amsterdam, Nieuwe Achtergracht 166, 1018 WV Amsterdam, The Netherlands

J. H. M. van den Berg**

Laboratory of Instrumental Analysis, Eindhoven University of Technology, P.O. Box 513, 5600 MB Eindhoven, The Netherlands

Key Words

HPLC
Heat transport equation
Temperature effects
Viscous heat dissipation

Summary

Temperature effects in HPLC columns due to viscous heat dissipation are examined. For the case when the thermostatted column wall and mobile phase at the column inlet are at the same temperature an explicit solution of the heat transport equation is given. The predicted temperature profile is parabolic at large distances from the column entrance; the magnitude of the effect is proportional to the square of the mobile phase velocity, and is of the order of a few degrees centigrade. At the upper end of the column a relaxation occurs over a length of a few centimers. Experimental results confirm the validity of the predictions made and indicate that the various assumptions and approximations are justified. Plate height curves obtained with two mobile phases with differing viscosities show a much smaller efficiency for the less viscous mobile phase. The curves show an upward curvature at high reduced velocities. Both phenomena can be related to thermal effects. It is concluded that viscous heat dissipation constitutes an obstacle to obtaining higher speed and efficiency in HPLC by the use of smaller particles. Possible remedies, such as the use of smaller bore columns or special thermostatting devices, look troublesome from the experimental point of view.

Introduction

One of the advantages of liquid chromatography as compared to gas chromatography is the mild temperature at which the experiments can be carried out. In recent years, however, a number of papers have appeared in which it was indicated that columns temperatures above ambient can lead to better results, such as improved resolution or shorter separation times. In ion-exchange chromatography especially the beneficial effect of temperature increase was found to be significant [1, 2]. Some authors have used the column temperature to optimize separations in liquid-solid chromatography [3, 4].

Apart from the influence of a change in the mean column temperature on the various chromatographic parameters, attention should be given to the effect of longitudinal and radial temperature gradients, brought about by the viscous heat dissipation, on the chromatographic performance. Halász [5] calculated the total temperature rise in an adiabatic column. This depends exclusively on the pressure drop and the specific nature of the mobile phase (density and specific heat capacity). Such calculations give an idea of the order of magnitude of the effect; but are not very relevant for the practice of chromatography, as the adiabatic case is hardly ever approached in reality. Columns as used in HPLC have a relatively fast heat exchange with ambient air and moreover they can be easily thermostatted in many instruments. In that case at least, the column wall is at controlled temperature. However, a radial temperature profile will develop then, as Horvath [6] indicated. This radial profile can affect chromatographic efficiency much more seriously than the longitudinal gradients.

In this paper we present some calculations and experimental results pertaining to these temperature effects, considering the shapes of the profiles as well as the magnitude of the temperature increase. A brief qualitative discussion of the effect on the chromatographic efficiency is given also.

Theoretical

The heat balance for an infinitesimal volume element of the column content can be given in cylindrical coordinates as:

$$\overline{dc}\,\frac{dT}{dt} = \bar{\lambda}_{lon}\frac{d^2T}{dz^2} + \bar{\lambda}_{rad}\left(\frac{d^2T}{dr^2} + \frac{1}{r}\frac{dT}{dr}\right) - v_s d_m c_m \frac{dT}{dz} + v_s \frac{dp}{dz} \qquad (1)$$

* Present address: Institute of Analytical Chemistry, University of Vienna, Währingerstraße 38, A-1090 Vienna, Austria

** Present address: DSM Research, P.O. Box 18, 6160 MD Geleen, The Netherlands.

0009-5893/81/9 0515-09 $ 02.00/0

in which

$\overline{dc}$ average heat capacity per volume for the heterogeneous system consisting of stationary bed and mobile phase, equal to $\sum_n \epsilon_n d_n c_n$ where ϵ_n, d_n and c_n indicate volume fractions, densities and specific heat capacities, respectively, of the various phases n in the column,

T temperature,

r distance from column axis,

z coordinate in the direction of the column axis, being zero at the column entrance,

$\bar{\lambda}_{lon}$ average effective heat conductivity of the column content in the longitudinal (z) direction,

$\bar{\lambda}_{rad}$ average effective heat conductivity of the column content in the radial (r) direction, including the convective contribution to heat transport.

$d_m c_m$ heat capacity per unit of volume of mobile phase.

v_s superficial flow velocity (volume flow rate divided by *total* cross section area of column),

p pressure (the dependence of dp/dz on the mobile phase velocity and the particle size is substituted in a later stage).

Eq. (1) is valid under the following conditions and assumptions:

- the mobile phase compressibility and its effect on the heat generation term (v_s dp/dz) can be neglected. This is an excellent approximation for liquids;
- heat transport in the heterogeneous system in radial and longitudinal directions can be described by effective heat conductivities. This is usually assumed and it corresponds to the description of mass transport with plate height or dispersion coefficient;
- the mobile phase velocity does not depend on the position in the column (v_s is taken as a constant). This is the case if the mobile phase can be considered as incompressible and if the column is well packed (plug flow).

The heat generation term v_s dp/dz (units $W m^{-3}$) can be derived by considering the work exerted by the pressure on the rear and front faces on an infinitesimal volume element, or, macroscopically, by considering that the total amount of pumping power, equal to $w \Delta p$, where w is the flow rate and Δp is the pressure drop, is dissipated in a uniform way over the total volume of the column.

The initial and boundary conditions determining the solution of eq. (1) are dependent on the experimental circumstances. As boundary conditions we take:

$$\left.\begin{array}{ll} z = 0 & T = T_e \\ \left.\begin{array}{l} 0 < z < L \\ r = R \end{array}\right\} & T = T_e \end{array}\right\} \qquad (2)$$

in which R and L are the internal radius and the length of the column respectively, and T_e is the temperature of the incoming mobile phase and the column wall. These conditions correspond to the case where the temperature of the column wall and the mobile phase are maintained by the same thermostat. Such conditions, apart from being usual, have the additional advantage for the present discussion that the thermal situation is better defined than in other cases, such as the operation of columns without any temperature control.

It is further assumed that the resistance to heat transfer in the column wall material can be neglected. Although the most usual material (ss 316) has a rather low thermal conductivity compared to other metals, the value ($90 W m^{-1} s^{-1} 0C^{-1}$) is still large enough to make this assumption quite realistic.

The problem of the initial conditions can be handled by limiting the discussion to the situation prevailing when the column has been operated for a sufficiently long time, avoiding stop flow techniques. For that case the temperature in any point in the column will be independent of time and we can equate the LHS of eq. (1) to zero.

Further simplification can be obtained by considering the situation for sufficiently large values of z. (There is no need in this context to limit z in the mathematical approach to values smaller than L.) For these values the terms in d^2T/dz^2 and dT/dz can be neglected, because ultimately the temperature will not depend on z. The resulting differential equation contains only r as the position coordinate and can be easily solved. The result which observes the boundary condition is: $T = T_e$ for $r = R$, is:

$$T(r, z = \infty) = T_e + \Delta \left(1 - \frac{r^2}{R^2}\right) \qquad (3)$$

where

$$\Delta = \frac{v_s \frac{dp}{dz} R^2}{4 \bar{\lambda}_{rad}}$$

Substituting

$$T(r,z) = T(r, z = \infty) + S(r,z)$$

into eq. (1) we obtain the less complex equation in S:

$$\bar{\lambda}_{lon} \frac{d^2S}{dz^2} + \bar{\lambda}_{rad} \left(\frac{d^2S}{dr^2} + \frac{1}{r}\frac{dS}{dr}\right) - v_s d_m c_m \frac{dS}{dz} = 0 \qquad (4)$$

where S should fulfill the boundary condition:

$$\left.\begin{array}{ll} z = 0 & S = -\Delta \left(1 - \frac{r^2}{R^2}\right) \\ \left.\begin{array}{l} 0 < z < L \\ r = R \end{array}\right\} & S = 0 \end{array}\right\} \qquad (5)$$

The solution (3) describes the situation prevailing at sufficiently large values of z. There the heat produced is completely conducted to the wall; the temperature depends on r exclusively. The temperature in eq. (3) is described by a parabolic function. However, for $z = 0$ the temperature must be equal to T_e according to eq. (2). The function S describes the relaxation with increasing z of the temperature function from the value T_e at $z = 0$ to the parabolic profile (3).

Eq. (4) is simplified by introducing dimension less variables ρ and ξ and a number M:

$$\left.\begin{aligned} \rho &= \frac{r}{R} \\ \xi &= z\,\frac{\bar{\lambda}_{rad}}{v_s d_m c_m R^2} \\ M &= \frac{\bar{\lambda}_{rad}\,\bar{\lambda}_{lon}}{v_s^2 d_m^2 c_m^2 R^2} \end{aligned}\right\} \qquad (6)$$

leading to:

$$M\frac{d^2S}{d\xi^2} + \frac{d^2S}{d\rho^2} + \frac{1}{\rho}\frac{dS}{d\rho} - \frac{dS}{d\xi} = 0 \qquad (7)$$

Solution of this equation along the usual lines, including separation of variables and expansion in Bessel functions and taking into account the boundary conditions yields*:

$$S = \Delta \sum_{s=1}^{\infty} \frac{8}{\lambda_s^3 J_1(\lambda_s)} J_0(\lambda_s \rho)\, e^{\frac{1-\sqrt{1+4M\lambda_s^2}}{2M}\xi} \qquad (8)$$

in which

λ_s the s'th root of the Bessel function of the first kind and zero order,

J_0 the same Bessel function,

J_1 the Bessel function of the first kind and first order.

In all practical cases M is small compared to unity. This corresponds to a small value of the $\bar{\lambda}_{lon}$ term in eq. (1). Using this for approximating the exponential function in eq. (8) by $e^{-\lambda_s^2 \xi}$, and back substituting the original variables results in the following expression for the total temperature profile:

$$T(r,z) = \frac{v_s \frac{dp}{dz} R^2}{4\bar{\lambda}_{rad}} \left(1 - \frac{r^2}{R^2} + \sum_{s=1}^{\infty} \frac{8\,J_0(\lambda_s \frac{r}{R})}{\lambda_s^3 J_1(\lambda_s)} e^{-\frac{\lambda_s^2 \bar{\lambda}_{rad} z}{v_s d_m c_m R^2}}\right) + T_e \qquad (9)$$

Although eq. (9) seems quite impractical, the main characteristics of the temperature profile can be readily extracted from it:

a) The maximum temperature rise, Δ, along the axis of the column, obtained at large values of z has already been given as:

$$\Delta = \frac{v_s \frac{dp}{dz} R^2}{4\bar{\lambda}_{rad}} \qquad (10)$$

Substitution of the Darcy equation for the pressure gradient, expressing v_s in the more usual migration velocity u_0 of an unretained solute and then using the factor 1000 for the geometrical factor [5] in the expression for the permeability yields:

$$\Delta = 200\,\frac{u_0^2 \eta R^2}{\bar{\lambda}_{rad} d_p^2} \qquad (11)$$

* Details of such a calculation can be found in a paper by Hupe and Bayer [7] and in references [8–11].

in which η is the dynamic viscosity of the mobile phase and d_p is the particle size and in which $v_s = \epsilon_m u_0$ has been used and a value of 0.8 has been taken for the volume fraction of the mobile phase ϵ_m.

b) The length within which this situation is reached depends on the parameters occurring in the exponents in eq. (9). A characteristic length l_s can be derived for every term in the equation, within which this term declines in magnitude with a factor e. These l_s values of course depend on the term number s. The most important first term in the expansion of Bessel functions has a λ_s^2 value of approximately 6. Therefore for this term (the other terms decline in magnitude more rapidly) we have:

$$l_1 \cong \frac{v_s d_m c_m R^2}{6\bar{\lambda}_{rad}} \cong \frac{w d_m c_m}{18\bar{\lambda}_{rad}} \qquad (12)$$

It follows that the relaxation length depends exclusively on the flow rate and the properties of the mobile phase; it is independent of the column diameter at a fixed flow rate.

The mean temperature rise over the cross section of the column can be found from integration of eq. (9) over the cross section. With the same approximation of the exponentials as used above this results in:

$$\bar{T}(z) = \Delta\left(\frac{1}{2} - 16 \sum_{s=1}^{\infty} \frac{1}{\lambda_s^4} e^{-\lambda_s^2 \xi}\right) + T_e \qquad (13)$$

The mean temperature rise over the column, averaged over radius and length is found from integration of eq. (13) over ξ from 0 to ξ_L

$$\bar{\bar{T}} = \Delta\left(\frac{1}{2} + \frac{16}{\xi_L} \sum_{s=1}^{\infty} \frac{1}{\lambda_s^6} (e^{-\lambda_s^2 \xi_L} - 1)\right) + T_e \qquad (14)$$

in which ξ_L is the dimensionless column length

$$\xi_L = L\,\frac{\bar{\lambda}_{rad}}{v_s d_m c_m R^2} \qquad (15)$$

In the following we discuss the values of the parameters occurring for a normal, state of the art, analytical column:

$$\left.\begin{aligned} v_s &= 2 \cdot 10^{-3}\ m\,s^{-1} \\ \frac{dp}{dz} &= 10^8\ N\,m^{-3}\ (10\ bar\,cm^{-1}) \\ R &= 2.3 \cdot 10^{-3}\ m \end{aligned}\right\} \qquad (16)$$

The composite parameters $\bar{\lambda}_{lon}$ and $\bar{\lambda}_{rad}$ require some discussion. In the first place they are not the same because the flow induces a non-isotropic character to the heat conduction. $\bar{\lambda}_{rad}$ especially will be enlarged compared to the value for the quiescent situation, because heat transfer by convection occurs, resulting from a process comparable to eddy diffusion for mass transfer. The convectional heat transfer in the longitudinal direction, on the other hand, was taken into account explicitly in eq. (1). By analogy with mass transfer we put:

$$\bar{\lambda}_{rad} = \lambda_{rad}^c + \lambda_{rad}^e \qquad (17)$$

in which the superscripts c and e refer to the conductive and convective (eddy) part of the effective conductivity.

There is little experimental data about the magnitude of λ^e_{rad} in packed beds in the laminar flow region prevailing in chromatography. We therefore use the results pertaining to the radial plate height, which describes the analogous *mass* transfer. We are fairly confident about the reliability of the results considering the widespread and succesful use of the analogy between mass and heat transfer.

The convective part of the radial plate height is probably a function of the flow velocity, but for the present purpose we can neglect this and retain good accuracy. We use the result obtained by Knox [12, 13].

$$H^e_r = 0.06\, d_p \tag{18}$$

In heat transfer this corresponds* to:

$$\lambda^e_{rad} = 0.03\, d_p v_s d_m c_m \tag{19}$$

The conductive part of $\bar{\lambda}_{rad}$, λ^c_{rad}, is in itself a composite quantity, because the heterogeneous system in the column, consisting of mobile phase, packing material and eventually stationary liquid phase, shows a macroscopic heat conductivity which is a function of the conductivities of the phases and the geometric structure. Weighed normal averages as well as weighed harmonic averages are in use for the estimation in such systems (cf. ref. [14]).

At present we cannot give a definitive solution to this problem. However, a first approximation can radily be given. It is highly probable that in the column beds as applied in HPLC the conductivity will be mainly determined by the mobile phase. This occupies a fraction of 0.8 of the column volume. The conductivities of the solvents used in HPLC as mobile phase constituents, some of which are listed in Table I, are between 0.15 and 0.7 W m^{-1} °C^{-1}. These values are much larger than the conductivity due to the presence of the silica skeleton, which can be estimated from the value given for diatomite material in vacuum, being 0.012 W m^{-1} °C^{-1} [14].

As a first approximation it is therefore reasonable simply to substitute the value for the mobile phase in use, keeping in mind that the actual value may be somewhat higher. The massive silica material has a much higher conductivity of about 1.4 W m^{-1} °C^{-1}.

The region in which the convective radial heat transport will be small compared to the conductive transport can now be estimated from eq. (19). As long as

$$\frac{d_p v_s d_m c_m}{\lambda_m} < 3 \quad \text{or} \quad \frac{d_p u_0 \epsilon_m d_m c_m}{\lambda_m} < 3$$

the error on neglecting λ^e_{rad} will be smaller than 10%.
The above condition can be rewritten as:

$$\nu < 4\, \frac{\lambda_m}{d_m c_m D_i} \tag{20}$$

in which

ν the reduced velocity referred to particle size as used by Knox, equal to $\frac{v_s d_p}{\epsilon_m D_i}$,

D_i the diffusion coefficient of the solute i in the mobile phase,

λ_m the heat conductivity of the mobile phase.

Table I lists the values of ν, ν^+, below which we can neglect λ^e_{rad} to a first approximation. It can be concluded from this table that only at very high values of ν do we have to take the convective transport into account. For preparative columns these reduced velocities may occur, for analytical columns they do not. Restricting the further discussion to analytical column we can consider the values for two frequently used mobile phase constituents, hexane and water, being 0.12 and 0.60 W m^{-1} °C^{-1} respectively.

With the chromatographic parameters as assumed above [eq. (16)] and using eq. (10) we obtain for hexane:

$$\Delta = 2.1\ °C$$

and for water.

$$\Delta = 0.44\ °C$$

For the relaxation length l_1 we obtain for these two solvents:

$l_1 = 1.9 \cdot 10^{-2}$ m for hexane and
$l_1 = 1.2 \cdot 10^{-2}$ m for water.

Fig. 1 shows the calculated radial temperature profile for a column with the parameters as assumed above, giving results for the two solvents, while the results are also expressed in the dimensionless parameters, $T-T_e/\Delta$ and ξ.

Fig. 2 shows the calculated results for the longitudinal profile for various radial positions in the column and for the temperature averaged over the column cross section [eq. (13)].

The effect exerted by the radial and longitudinal temperature profile on the chromatographic peak shapes, that

Table I. Thermal parameters of common liquids used as mobile phase constituents in HPLC

	Heat capacity per volume 10^6 J m^{-3} °C^{-1}	Thermal conductivity W m^{-1} °C^{-1}	Diffusion coefficient (Wilke-Chang) M = 200 10^{-9} m^2 s^{-1}	ν^+ –
Water	4.19	0.60	0.60	930
Methanol	1.99	0.21	1.14	370
Ethanol	1.92	0.18	0.60	630
Propanol-1	1.97	0.17	0.46	740
Acetonitrile	1.78	0.19	1.80	240
Diethylether	1.61	0.14	3.22	110
Dichloro-methane	1.59	0.14	1.79	200
Chloroform	1.44	0.12	1.64	230
Ethylacetate	1.73	0.14	1.80	220
Hexane	1.46	0.12	2.48	160
Pentane	1.39	0.11	3.10	130
Acetone	1.75	0.16	2.10	200

* The figure corresponds to a Pe' number (terminology of ref. [8]) of 30, which seems to be rather high compared to values given in ref. [8] for heat and mass transfer. We prefer to use Knox's value, in other words we prefer the actual measured value for a *microparticulate*, bed, be it for mass transfer, to the extrapolations from large scale measurements with high Re numbers to HPLC systems.

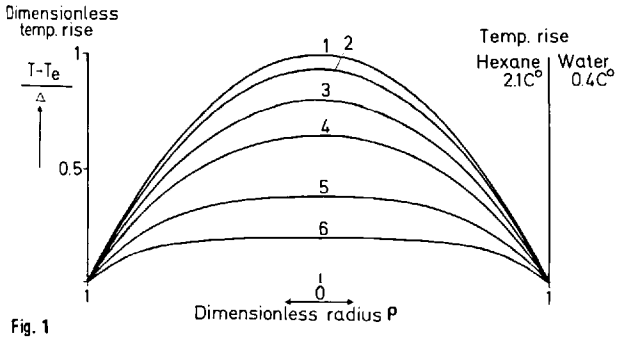

Fig. 1

Calculated dependence of temperature rise, $T-T_e$, on radial position, ρ, in column for various longitudinal positions, ξ, in column. 1: $\xi > 1$; 2: $\xi = 0.5$; 3: $\xi = 0.3$; 4: $\xi = 0.2$; 5: $\xi = 0.1$; 6: $\xi = 0.05$. These ξ values according to eq. (15) correspond to distances from top of column of 56 mm, 34 mm, 23 mm, 11 mm and 5.6 mm for hexane as eluent and of 36 mm, 22 mm, 14 mm, 7.3 mm and 3.6 mm for water as eluent, under conditions described in eq. (19). Absolute temperature increase indicated on ordinate on left hand side also applies to conditions of eq. (16).

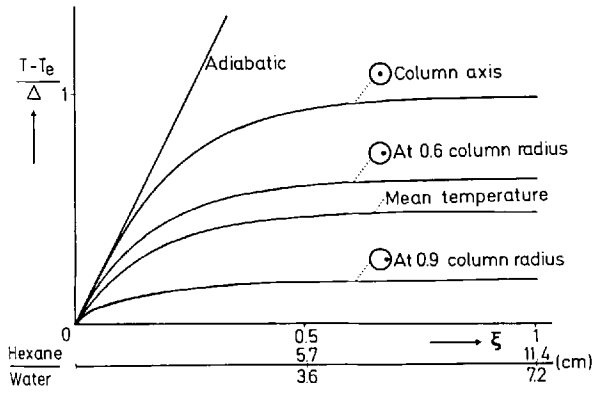

Fig. 2

Calculated dependence of temperature rise, $T-T_e$, on longitudinal position, ξ, in column for various radial positions, ρ, and for mean. Plot also applies to conditions of eq. (16).

is, the elution function of solutes, will be rather complicated to describe and this effect will be dealt with in future papers. However, a few general and semi-quantitative considerations will be given here.

The inhomogeneous temperature and the average temperature rise will affect the migration rates in numerous ways. In the first place the volume of the whole column as well as the volumes of the various phases may change, as a result of thermal expansion. Even more complicated changes in the geometry of the column content may occur when the mutual solubility of the phases changes strongly with temperature.

However, with the packings and phases most popular these days, namely, various kinds of chemically modified or unmodified silica materials used as adsorbent packings, these effects will be small compared to those brought about by the changes in viscosity and distribution constants.

The change in viscosity will lead to different mobile phase velocities for the various radial positions in the column. The mean velocity, however, will be hardly affected, provided constant flow pumps are used. It follows that the viscosity change will not strongly influence the mean residence time of solutes. This holds even more for the retention parameters derived from the retention times, such as capacity factors and relative retention, because cancellation of the effect will occur.

These latter parameters are especially influenced via the temperature dependence of the distribution constants. For numerous phase systems, which are based on physical distribution only, the temperature dependence of the distribution constants is about 2% per degree centigrade. For those systems it can therefore be concluded that the viscous heat dissipation will affect the accuracy of retention data to the extent of a few percent. On the other hand, numerous phase systems in which chemical reactions are involved in the distribution process show a much stronger temperature dependence [15, 16], and very significant systematic error may occur with such systems.

The peak broadening effect in state-of-the-art HPLC columns may be significantly influenced by the radial temperature profile. Consider the asymptotic profile of parabolic shape, with a maximum deviation along the column axis of a few degrees centigrade.

As a first approximation, assuming a linear dependence of the viscosity on the temperature, the situation can be described by a parabolic velocity profile, with a maximum deviation in the column axis amounting to a few percent, as the viscosity changes by about 2% per degree. Radial diffusion or dispersion of the solute will counteract the peak broadening effect associated with this profile, just as in the case of dispersion in open tubes described by Aris [17] and Taylor.

With the use of smaller particles heat production increases and radial dispersion of solutes decreases [12, 13]. It follows that the detrimental effect of viscous heat dissipation on efficiency will be especially large with smaller particles and it can be expected that the thermal effect will play a dominant role in the exploration of the possibilities of particles smaller than 5 μm for obtaining higher speeds and efficiencies.

At first sight four solutions can be suggested, neither of which looks very attractive from the practical point of view.

a. Use of temperature-controlled columns with smaller diameters.
The strong influence of the column radius as expressed in eq. (10) guarantees the elimination of the thermal disturbance in this way. However, this approach presents tremendous difficulties with regard to injection and detection instrumentation, because the peak volume standard deviations obtained with efficient columns with small particles and small diameters will be very small.

b. Use of adiabatic columns.
Accepting the longitudinal profile and corresponding change in distribution, this approach would allow for homogeneous migration and therefore for high efficiency. The realization of this concept is, however, more difficult than might be expected. It requires a column wall material of low thermal conductivity, in combination with chemical inertness and mechanical strength. With

stainless steel as the wall material, which has a conductivity of 90 $W m^{-1} °C^{-1}$, an attempt to operate a column adiabatically would lead to a flow of heat through the column wall, from bottom to top, generating parabolic profiles of opposite signs at both ends of the column.

A solution of this problem might be envisaged in thermostatting the column wall material in such a way that the linear adiabatic profile along the column length would not be disturbed by heat transfer to the wall. A similar system is sometimes used with destillation columns. The temperature of the column wall should be forced into a linear longitudinal profile, with a slope equal to that followed by the column content. Complexity of LC systems would increase considerably.

c. Use of the infinite diamter concept as proposed by Knox [14, 15].

By designing columns and injection devices in such a way that the solutes are confined to a relatively narrow central core of the column the influence of the temperature profile is diminished considerably. We do not exclude the possibility that the success of this concept as observed in numerous cases is at least partly connected with the thermal gradient, and not exclusively with the wall effects in permeability and packing structure.

In the opinion of the present authors the use of the infinite diameter concept involves compromises with respect to other important analytical characteristics of the HPLC system, such as detection limit, reproducibility and simplicity of instrumentation.

d. Refraining from the use of high pressures.

This approach, as proposed by Guiochon and coworkers [18], carefully optimizing particle diameter and column length within a constraint of a pressure drop of a few bar, would remove the whole problem with the temperature profile. However, although it is probable that performance with respect to speed and efficiency in this way can be virtually the same as that obtained with many HPLC columns in use nowadays, it is hard to see how a further increase in speed of separation can be obtained without the use of high pressures.

It can be concluded that, apart from other difficulties, the prospects for HPLC with particles wall below 5 μm do not look very promising, because of thermal effects. This would mean that the trend toward smaller particles has to stop at a limit to be met earlier than the limit indicated by Knox and Saleem [19] in their optimization equations, which were derived without taking the thermal effects into account. Only concurrent use of smaller column diameters or similar measures, necessitating a drastic change in the whole HPLC technology, would be sufficient to avoid this problem.

Experimental

Equipment

The following columns were used.

A. Stainless steel column 20 cm x 4.6 mm i.d., containing 8 thermocouples at various longitudinal positions, positioned as precisely as possible (± 1 mm) in the column axis. Column packing silica LiChrosorp Si 60 (E. Merck, Darmstadt, FRG), mean particle size of about 5 μm. Column A was used for the measurement of the axial column temperature.

B. Stainless steel columns of various dimensions packed with LiChrosorb Si 60 (E. Merck, Darmstadt) with a mean particle diameter of 6.5 μm, or alumina with a mean particle diameter of 1.8 μm (gift from prof. K.K.Unger, Darmstadt). These columns were used for the measurement of the temperature averaged over the flow cross section, the so-called cupmixing temperature, at the column outlet.

C. Thick-walled stainless steel column 25 cm x 10 mm o.d., and 4.6 mm i.d. (Knauer, Berlin, FRG), slurry packed with Hypersil ODS 5 μm (Shandon, Runcorn, Cheshire, UK). This column was used for the measurement of the theoretical plate height.

Column A was placed in a plastic cylinder about 5 cm diameter and thermostatted by means of a vigorous air stream of constant temperature. For heating, the air stream is led through 2 m of copper tubing immersed in a thermostatted water bath. This method was chosen in order to avoid electrical contact of the thermocouple wires with a thermostatting liquid.

For columns B thermostatting was accomplished by immersing the columns in a water bath; the outlet of the columns was held upwards and consisted of a capillary made of Kel F® instead of stainless steel as usual. A thermocouple was inserted into this capillary. The latter was positioned just above the level of the thermostatting liquid, while the column terminator was immersed. This procedure was chosen in order to thermostat the full column length, while avoiding further thermostatting of the mobile phase in the outlet capillary.

Column C was thermostatted by means of a water jacket.

The measuring equipment consisted of a potentiometric recorder of 20 μV maximum full scale sensitivity (Kipp en Zonen, Delft, The Netherlands, type BD 5) for the thermocouple measurements, a fixed wavelength UV-detector (Waters, Framingham, MA, USA, type M 6000) for the plate height measurements.

A reciprocating pump (Orlita, Gießen, FRG, type AE 1500), fitted with an effective pulse damping system (custom made), and a pressure intensifier pump (Haskell, Burbanks, CA, USA, type DST 150 A) were used for the temperature measurements at low and high pressures respectively and a syringe type pump (Varian, Palo Alto, CA, USA, type 8500) for the plate height measurements, the latter in combination with a sampling valve (Rheodyne, Berkeley, CA, USA, type 7120), fitted with a loop of 10 μl.

Chemicals

Iso-octane was used as the mobile phase for columns A and B. Mixtures of acetonitrile and water and of ethanol and water were used as the mobile phase for column C. Nitrobenzene and uracil were used as retained and unretained compound respectively. All chemicals were of analytical reagent grade and used as delivered.

Results and Discussion

Longitudinal Increase of Axial Temperature

Column A was operated as indicated above. In the first place the velocity of the air stream was varied in order to find out whether resistance to heat transfer in the air played an important role. This was found not to be the case at the lower eluent flow rates, while at very high eluent flow rates a slight effect was observed. The highest air flow rate possible, 1 $l\,s^{-1}$, was used in further experiments.

Fig. 3 shows measured values for the axial temperature increase, ΔT, as a function of the longitudinal position in the column, for four mobile phase flow rates. The final axial temperature increase for 100 bar pressure drop, for example is observed to be about 1 °C. Calculation according to eq. (10) yields a result of 0.84 °C for these conditions.

The relaxation length l_1 can be read best from the 150 bar plot and is observed to be about 2 cm. Calculation according to eq. (12) gives 1.8 cm.

Mean Outlet Temperature Increase

In a second set of experiments the mean or cupmixing temperature increase of the mobile phase at the outlet of the column was measured using columns B. Fig. 4 shows the results for a number of columns of different geometry.

On the abscissa the value of $v_s \frac{dp}{dz} R^2 = \frac{w\,\Delta p}{\pi L}$ is used in accordance with eq. (10). It can be seen that the points lie on a straight line for the lower values of the abscissa. The Figs. 4 a–c also show for the silica columns the temperature increases as calculated by eq. (9) with a value of $\bar{\lambda}_{rad}$ equal to that of the mobile phase, 0.146 W m^{-1} $°C^{-1}$. In view of the uncertainties connected with this latter assumption the agreement between calculated and observed temperature increase is considered to be very satisfactory for the silica columns at low abscissa values.

The agreement between calculated and observed temperature increase is less good for higher pressures. This is not surprising, considering that a number of explicit or tacit assumptions in the theoretical derivation are not completely valid in the real situation:

- the permeability of the real column is highly independent of the radial position, because any deviation from this would be apparent in the theoretical plate height, but it is not certain that the permeability is constant over the column length;
- the viscosity of the mobile phase, and therefore the pressure gradient, changes throughout the columns as a result of the pressure and temperature dependence of the viscosity. These second order effects will be of larger importance at the higher flow rates and pressures;
- the compressibility of the mobile phase probably can not be neglected at the rather drastic conditions at the higher pressures. Heat effects associated with decompression, removing some of the friction heat*, play a role then.

For the column packed with 1.8 μm alumina particles the agreement between calculated and measured values is less good: observed temperature increases are about half the calculated values. We suspect that the abnormal behaviour of this column is caused by the higher volume fraction of the base material in this packing and to the higher thermal conductivity of the massive base material as compared to silica (21 W m^{-1} $°C^{-1}$ vs 1.4 W m^{-1} $°C^{-1}$). This makes less appropriate the assumption that the thermal conductivity of the column is determined predominantly by the mobile phase. The dashed line in Fig. 4d was calculated with an adapted value of 0.34 W m^{-1} $°C^{-1}$ for $\bar{\lambda}_{rad}$. Unfortunately silica particles of this size were not available.

There are some experimental difficulties involved in measuring the cupmixing temperature:

- further thermostatting of the mobile phase in the outlet capillary cannot be excluded completely;
- some heat will be transported by the thermocouple wires;
- it is not certain in the cupmixing temperature experiments that the measurement is accurate, because thermal homogeneity may not yet have been reached.

In view of all these difficulties the theoretical interpretation of the experimental data may be considered to be quite satisfactory.

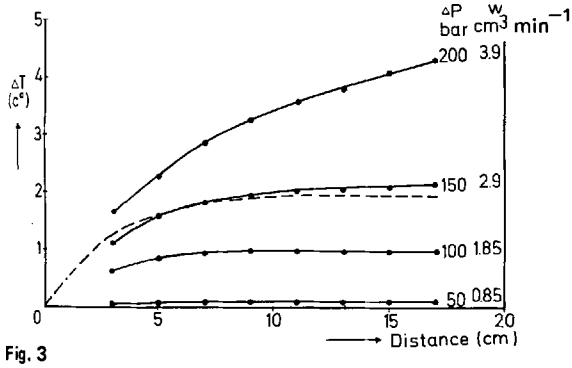

Fig. 3

Observed dependence of axial temperature rise, $\Delta T = T - T_e$, on longitudinal position in column.

Column 200 mm x 4.6 mm i.d., packing 5 μm silica, operated at 50; 100; 150 and 200 bar inlet pressure. Flow rates w indicated in ml/min correspond to retention times of unretarded peaks of 20.3s, 28.9s, 39.3s and 59.5s.

Dashed line gives results of prediction according to eq. (9) with $\lambda_{rad} = \bar{\lambda}_m$ for 150 bar experiment.

Relationship Between Axial and Cupmixing Temperature

Fig. 5 shows the results of cupmixing and axial temperature measurements, obtained with column A. As can be seen the cupmixing temperature increase is about half the value for the increase in the column axis, as obtained by extrapolating the temperatures measured by the thermocouples to the position $z = 20$ cm, being the end of the column (Fig. 3). This agrees exactly with the theoretical treatment.

It can be concluded that the dependence of the temperature in the HPLC column on the radial and longitudinal position

* In gas chromatography at higher pressure drops heat of friction and heat absorbed by decompression cancel exactly as long as the carrier gas can be considered as ideal. In fact the Joule-Thomson experiment is being repeated. We thank R. J. Jonker for pointing this out.

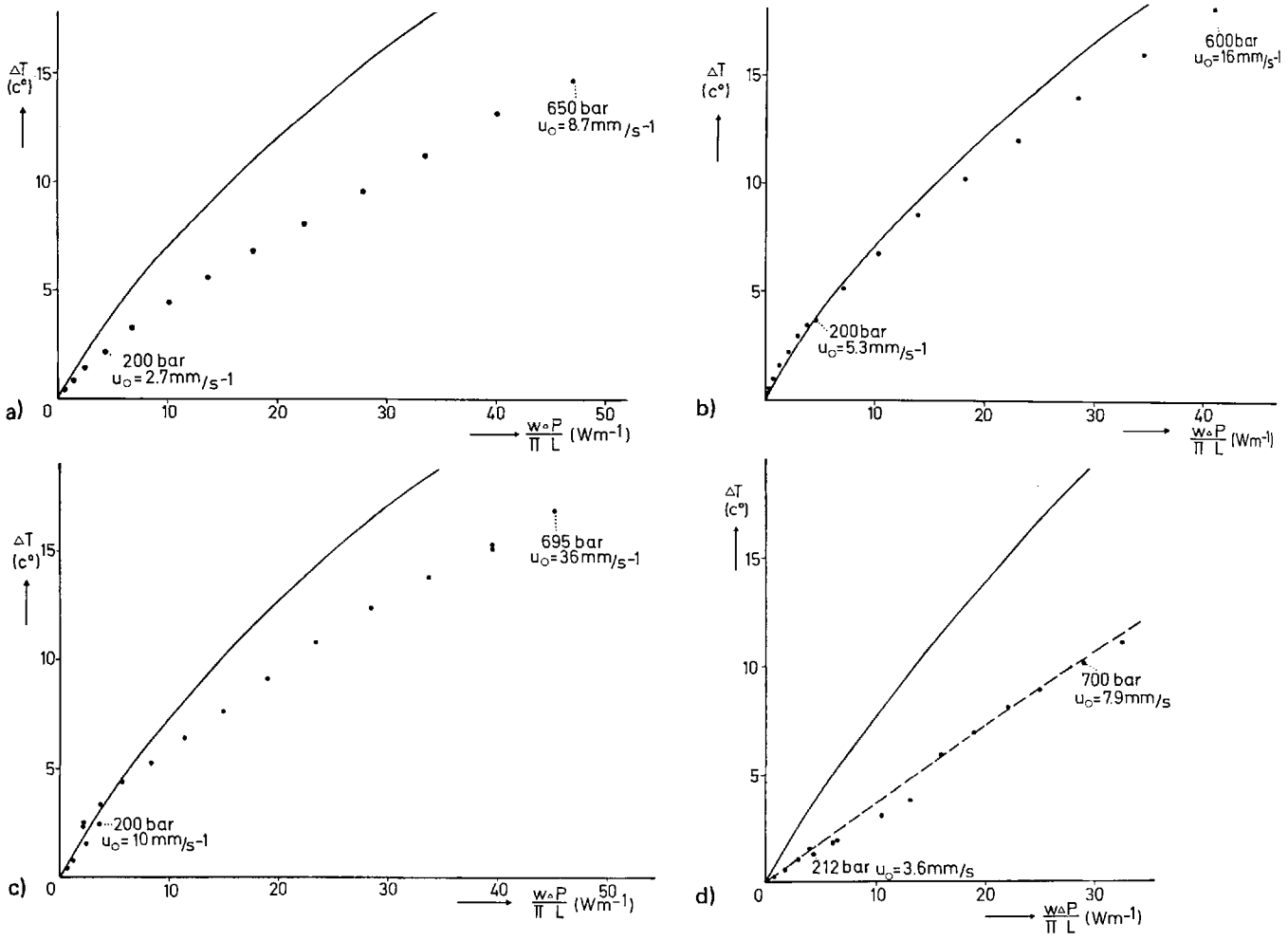

Fig. 4

Observed (•) and calculated (——) mean outlet eluent (cupmixing) temperature increases plotted as function of heat dissipation per unit length over π. Pressure drop Δp in bar or N m^{-2}, flow rates w in $m^3 s^{-1}$, length L in m, velocity u_0 of the unretained compound in mm s^{-1}.

Columns: a: 100 x 3 mm i.d., packing silica 5 µm; b: 100 x 4.6 mm i.d., packing silica 5 µm; c: 100 x 10 mm i.d., packing silica 6.5 µm; d: 100 x 4.6 mm i.d., packing alumina 1.8 µm. Iso-octane was used as eluent in all cases.

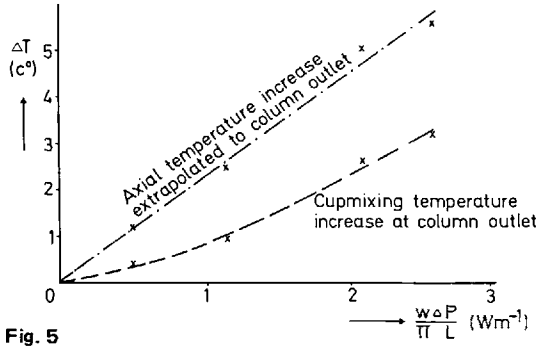

Fig. 5

Observed mean outlet eluent (cupmixing) temperature increases and axial temperature increases extrapolated to end of column plotted as function of heat dissipation per unit length over π.

Column A, fitted with thermocouples, 200 x 4.6 mm i.d., packing silica 5 µm, eluent iso-octane.

is satisfactorily described by eqs. (9), (10) and (12). The radial thermal conductivity can be approximated well by that of the mobile phase in the case of silica columns; for alumina columns a higher value must be assumed.

Effect of Axial Temperature Profile on Theoretical Plate Height

As was discussed in the theoretical section the radial temperature profile can be expected to exert a large influence on the column efficiency. The effect may perhaps be a clue to the high reduced plate heights and high slopes in log h vs log ν plots found by Unger et al. [18] for particle diameters below 4 µm. Experimental proof of such a conjecture is difficult to give, however.

A change in the column diameter [cf. eq. (10)] in principle provides a method for influencing the magnitude of the temperature profile. However, in view of the uncertainties connected with the packing geometry, the interpretation of the results of theoretical plate height measurements in wide bore and small bore columns would be questionable. Other ways to approach the problem, namely, the use of stream splitting devices at the column end or special thermostatting arrangements are presently not available to the authors.

We decided to carry out an experiment in which the same column was operated with two mobile phases of significantly different viscosity, resulting in different tem-

perature deviations between wall and core of the column, for the same linear flow velocity [cf. eq. (11)].

In order to facilitate the interpretation the mobile phases were chosen so as to give about the same capacity factor for the same solute. However, the interpretation nevertheless is complicated.

In the first place the theoretical plate height, as determined in the usual way via the peak width at 0.6 maximum height, is probably not very sensitive to the radial temperature profile because the parabolic shape of the latter leads to a fairly uniform temperature in a relatively large central core of the column; only the wall region deviates significantly in temperature from the axial region. Thus it can be expected that the temperature effect leads rather to tailing peaks than to symmetrical peak broadening.

In the second place the change in mobile phase viscosity is accompanied by a change of similar relative magnitude but in the opposite direction in the diffusion coefficient (Wilke Chang [21]). Plate heights measured in the two mobile phases will thus differ already on the basis of the usual theoretical plate height equations for chromatography [22, 23], as these indicate a dependence of the reduced plate height, $h = H/d_p$, on the reduced velocity $\nu = u_0 d_p/D_i$, where D_i is the diffusion coefficient in the mobile phase. The comparison should therefore be made at the same value for the reduced velocity. It should be noted that the operation at the same reduced velocity with different mobile phases results in about the same pressure drop, as long as the Wilke Chang equation is obeyed. For which mobile phase the strongest temperature effect will develop then depends also on the thermal conductivities of the two solvents. Usually, however, the one with the smallest viscosity will give the largest temperature effect.

Fig. 6 shows h vs ν curves obtained with column C with nitrobenzene as the solute. Ethanol–water (37.5% + 62.5% v/v) was one mobile phase, having a viscosity $\eta = 2.4\ 10^{-3}$ kg m^{-1} s, a thermal conductivity of $\lambda = 0.4$ W m^{-1} °C^{-1} and a capacity factor of 3.92 for nitrobenzene. The other mobile phase was acetonitrile–water (43.5% + 56.5% v/v), having a viscosity of $\eta = 0.75\ 10^{-3}$ kg m^{-1} s, a thermal conductivity of $\lambda = 0.4$ W m^{-1} °C^{-1} and a capacity factor of 3.60. Viscosities and thermal conductivities were estimated according to ref. [24]. The temperature deviations for the two mobile phases are predicted by eq. (10) to be in the ratio 6:1 at the same reduced velocity.

The theoretical plate heights shown in Fig. 6 were determined from the peak widths at 0.1 maximum peak height. The reduced plate height, h, with acetonitrile–water, with which the biggest temperature effect occurs, is indeed much larger than that observed with methanol–water. The ratio of the two reduced plate heights increases with increasing reduced velocity. Moreover, both lines show an upward curvature. All this is to be expected when the temperature effect plays an important role in the efficiency.

As external effects outside the column could bring about similar phenomena, these were determined in a separate experiment in which the injector was directly connected to the detector. The error in the plate heights due to these extra column effects was found to be smaller than a few percent in all cases.

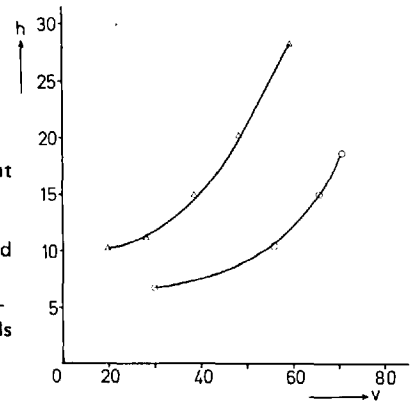

Fig. 6
Plot of reduced plate height vs reduced velocity for thermostatted column C with ethanol–water (○) and acetonitrile–water (△) as mobile phase. Solute nitrobenzene. For further details see text.

Acknowledgement

Thanks are due to Mr. F. Nooitgedagt, Mr. J. J. Blom and Mr. W. Markovski for valuable contributions to the experimental work and to Mr. K. Camstra for the construction of parts of the equipment. Prof. Dr. J. M. H. Fortuin is acknowledged for a stimulating discussion on theoretical aspects of this paper.

References

[1] *C. G. Horvath, B. A. Preiss* and *S. R. Lipsky*, Anal. Chem. 39, 1422 (1967).
[2] *P. R. Brown*, J. Chromatogr. 52, 257 (1970).
[3] *J. A. Schmidt, R. A. Henry, R. C. Williams* and *J. F. Dieckman*, J. Chromatog. Sci. 9, 645 (1971).
[4] *J. R. Gant, J. W. Dolan* and *L. R. Snyder*, J. Chromatogr. 185, 153 (1979).
[5] *I. Halász, R. Endele* and *J. Asshauer*, J. Chromatogr. 112, 37 (1975).
[6] *C. G. Horvath* and *H. J. Lin*, J. Chromatogr. 149, 43 (1978).
[7] *K. P. Hupe* and *E. Bayer* in *A. Goldup* (ed.), Gas Chromatography 1964, Institute of Petroleum, London 1965, p. 62.
[8] *E. Singer* and *R. H. Wilhelm*, Chem. Engin. Progress 46, 343 (1950).
[9] *M. S. Brinn, S. J. Friedman, F. A. Gluckert* and *R. L. Pigford*, Ind. Engin. Chem. 40, 1050 (1948).
[10] *W. Jost*, Diffusion in Solids, Liquids, Gases, in *E. Hutchinson* and *P. van Rysselberghe* (ed.), Physical Chemistry, vol. I, New York 1960.
[11] *A. Gray* and *G. B. Mathews*, A treatise on Bessel Functions and their Applications to Physics, Dover Publications, New York 1966.
[12] *D. Horne, J. H. Knox* and *L. McLaren*, Separ. Sci. 1, 531 (1966).
[13] *J. H. Knox, G. R. Laird* and *P. A. Raven*, J. Chromatogr. 122, 129 (1976).
[14] *M. Jakob*, Heat Transfer, vol. I and II, John Wiley and Sons, New York, 1965.
[15] *J. C. Kraak* and *J. F. K. Huber*, J. Chromatogr. 102, 333 (1974).
[16] *C. P. Terwey-Groen* and *J. C. Kraak*, J. Chromatogr. 138, 245 (1977).
[17] *R. Aris*, Proc. Roy. Soc., London Ser. A 235, 67 (1956).
[18] *M. Martin, C. Eon* and *G. Guiochon*, J. Chromatogr. 99, 357 (1974).
[19] *J. H. Knox* and *M. Saleem*, J. Chromatogr. Sci. 7, 614 (1969).
[20] *K. K. Unger, W. Messer* and *K. F. Krebs*, J. Chromatogr. 149, 1 (1978).
[21] *C. R. Wilke* and *P. Chang*, J. Am. Inst. Chem. Ingin. J. 1955, 264.
[22] *J. F. K. Huber*, Ber. Bunsenges. phys. Chem. 77, 179 (1973).
[23] *J. H. Knox*, J. Chromatogr. Sci. 15, 352 (1977).
[24] *R. C. Reid* and *T. K. Sherwood*, The properties of Gases and Liquids, McGrawHill, NY 1958.

Received: Feb. 9, 1981
Accepted: May 11, 1981
C